The zero-order regular approximation for relativistic effects: The effect of spin–orbit coupling in closed shell molecules

E. van Lenthe, J. G. Snijders, and E. J. Baerends
Afdeling Theoretische Chemie, Vrije Universiteit, De Boelelaan 1083, 1081 HV Amsterdam, The Netherlands

(Received 23 January 1996; accepted 5 July 1996)

In this paper we will calculate the effect of spin–orbit coupling on properties of closed shell molecules, using the zero-order regular approximation to the Dirac equation. Results are obtained using density functionals including density gradient corrections. Close agreement with experiment is obtained for the calculated molecular properties of a number of heavy element diatomic molecules. © *1996 American Institute of Physics.* [S0021-9606(96)02138-1]

I. INTRODUCTION

The zero-order regular approximation (ZORA)[1–3] to the Dirac equation has been successfully applied before[4] to molecules in the variant where spin–orbit interaction was neglected (which we will refer to as the scalar relativistic approximation).

The ZORA Hamiltonian is, in contrast to the Pauli Hamiltonian, regular at the origin even for a Coulombic potential. This is achieved by using an expansion in $E/(2c^2-V)$, which remains <1 close to the nucleus, instead of using $(E-V)/2c^2$, which leads to the Pauli terms but which diverges at the nucleus. The ZORA Hamiltonian was shown to give very accurate results in atomic calculations, especially for valence orbitals.[3] Exact solutions for the hydrogenic ions were given in Ref. 5 and it was shown there that the ZORA Hamiltonian is bounded from below for Coulombic potentials. The precise relation between the ZORA and the Pauli energies was recently studied in some detail.[6]

In this paper we will concentrate on the treatment of molecular spin–orbit effects by the full ZORA method. As before, we will use density functional theory, employing the usual (nonrelativistic) density functionals for the exchange–correlation energy: local density functionals (LDA) with gradient correction terms added, using the so-called generalized gradient approximation (GGA). The Becke correction for exchange[7] and the Perdew correction for correlation,[8] which have been successfully applied in nonrelativistic calculations[9,10] and in scalar relativistic ZORA calculations,[4] have been used.

In the double-group symmetry that applies in the presence of spin–orbit coupling, the molecules we are dealing with in this study are all closed shell. The Kohn–Sham one-electron method of density functional theory can thus be applied straightforwardly. For open shell atoms, however, the situation is more problematic. We discuss the problems that arise in this case in Sec. III. We propose an approximate way to deal with intermediate coupling in the density functional context, which we subsequently use to obtain the reference energies for the atomic ground states that are needed to calculate bond energies. In the appendix we also present results for some (excited) atomic multiplet energies using this method. In Sec. IV we analyze the spin–orbit effects on the closed shell molecules I_2, Au_2, Bi_2, HI, AuH, TlH, IF, TlF, TlI, PbO, and PbTe. These effects have been extensively studied before, especially within a relativistic effective potential framework (see, e.g., Refs. 11 and 12). In particular Pitzer[13,14] analyzed these effects in terms of the bonding between the spin–orbit split jj coupled atomic spinors of the constituent atoms. Here we will proceed slightly differently by treating the spin–orbit interaction as a modification on a scalar relativistic (*LS* coupled) starting point. Bond distances, harmonic frequencies, dissociation energies, and dipole moments are discussed. The results for the dissociation energies are very accurate if we include gradient correction (GGA) terms in the energy. Results for the dissociation energies are then usually within 0.1 eV of experiment, with only a few exceptions. The maximum deviation is 0.28 eV for PbO, and the average deviation is ~0.1 eV for this series of compounds. Bond distances and frequencies are not much affected by the spin–orbit coupling. Bond distances never change by more than 0.03 Å and for frequencies the effect is less than 10%.

Finally we compare our results to other relativistic treatments, including Dirac–Fock, relativistic effective potential, and Douglas–Kroll methods.

II. BASIC EQUATIONS

In this paper we will solve the ZORA equation, which is obtained as the zero-order equation in the regular expansion in $E/(2c^2-V)$ of the Dirac equation. The one-electron relativistic Kohn–Sham equations are solved in the scalar relativistic (SR) and in the fully relativistic case (including the spin–orbit operator). In this paper we will focus on the effects of spin–orbit coupling on molecular properties. The ZORA equation is

$$H^{\mathrm{ZORA}}\Phi^{\mathrm{ZORA}}=\left(V+\boldsymbol{\sigma}\cdot\mathbf{p}\,\frac{c^2}{2c^2-V}\,\boldsymbol{\sigma}\cdot\mathbf{p}\right)\Phi^{\mathrm{ZORA}}$$
$$=(H_{\mathrm{SR}}^{\mathrm{ZORA}}+H_{\mathrm{SO}}^{\mathrm{ZORA}})\Phi^{\mathrm{ZORA}}$$
$$=\left(V+\mathbf{p}\,\frac{c^2}{2c^2-V}\,\mathbf{p}+\frac{c^2}{(2c^2-V)^2}\,\boldsymbol{\sigma}\cdot(\boldsymbol{\nabla}V\times\mathbf{p})\right)\Phi^{\mathrm{ZORA}}$$
$$=E^{\mathrm{ZORA}}\Phi^{\mathrm{ZORA}}. \tag{1}$$

Here we see that the spin–orbit operator, in regularized form, is already present in this zero-order Hamiltonian. The potential V contains the nuclear field and the electron Coulomb and exchange–correlation potentials. The scalar relativistic ZORA equation is just the previous equation without the spin–orbit operator

$$H_{\mathrm{SR}}^{\mathrm{ZORA}}\Phi_{\mathrm{SR}}^{\mathrm{ZORA}}=\left(V+\mathbf{p}\,\frac{c^2}{2c^2-V}\,\mathbf{p}\right)\Phi_{\mathrm{SR}}^{\mathrm{ZORA}}$$
$$=E_{\mathrm{SR}}^{\mathrm{ZORA}}\Phi_{\mathrm{SR}}^{\mathrm{ZORA}}. \tag{2}$$

The one-electron energies can be improved using the so-called scaled ZORA energy, which sums certain higher order contributions to infinite order[5,15]

$$E^{\mathrm{scaled}}=\frac{E^{\mathrm{ZORA}}}{1+\langle\Phi^{\mathrm{ZORA}}|\,\boldsymbol{\sigma}\cdot\mathbf{p}\,\frac{c^2}{(2c^2-V)^2}\,\boldsymbol{\sigma}\cdot\mathbf{p}\,|\Phi^{\mathrm{ZORA}}\rangle}. \tag{3}$$

In an analogous way the scaled energy in the scalar relativistic case is

$$E_{\mathrm{SR}}^{\mathrm{scaled}}=\frac{E_{\mathrm{SR}}^{\mathrm{ZORA}}}{1+\langle\Phi_{\mathrm{SR}}^{\mathrm{ZORA}}|\mathbf{p}\,\frac{c^2}{(2c^2-V)^2}\,\mathbf{p}|\Phi_{\mathrm{SR}}^{\mathrm{ZORA}}\rangle}. \tag{4}$$

In practical implementations (in our case in ADF, the Amsterdam Density Functional program system) the one-electron wave functions (Kohn–Sham orbitals) are expanded in basis functions. In the ADF program Slater type orbital (STO) basis sets are employed. The SR ZORA equations lead to ''kinetic energy'' matrix elements between basis functions ϕ_i and ϕ_j of the form

$$\langle\phi_i|T_{\mathrm{SR}}^{\mathrm{ZORA}}|\phi_j\rangle=\langle\phi_i|\mathbf{p}\,\frac{c^2}{2c^2-V}\,\mathbf{p}|\phi_j\rangle$$
$$=\sum_k\left\langle\frac{\partial\phi_i}{\partial x_k}\left|\frac{c^2}{2c^2-V}\right|\frac{\partial\phi_j}{\partial x_k}\right\rangle, \tag{5}$$

where in the last step partial integration has been used. Usually the point group symmetry of the molecule is used to block diagonalize the Hamiltonian matrix. To this end, in the nonrelativistic and scalar relativistic cases a linear transformation is performed on the basis functions to an orthonormalized set of single group symmetry adapted functions.

In the fully relativistic case, where spin–orbit coupling is included, double group symmetry adapted functions have to be used. In this case one needs, apart from the SR ZORA ''kinetic energy,'' the ZORA spin–orbit matrix elements. In terms of double-group symmetry adapted functions ϕ_i^d and ϕ_j^d (two-component functions), the ZORA spin–orbit matrix elements are

$$\langle\phi_i^d|H_{\mathrm{SO}}^{\mathrm{ZORA}}|\phi_j^d\rangle=\langle\phi_i^d|\frac{c^2}{(2c^2-V)^2}\,\boldsymbol{\sigma}\cdot(\boldsymbol{\nabla}V\times\mathbf{p})|\phi_i^d\rangle$$
$$=\langle\phi_i^d|\boldsymbol{\sigma}\cdot\boldsymbol{\nabla}\left(\frac{c^2}{2c^2-V}\right)\times\mathbf{p}\rangle)|\phi_j^d\rangle$$
$$=\langle\phi_i^d\boldsymbol{\sigma}\cdot\boldsymbol{\nabla}\left(\frac{V}{4c^2-2V}\right)\times\mathbf{p}\rangle)|\phi_j^d\rangle$$
$$=i\sum_{lmn}\epsilon_{lmn}\left\langle\frac{\partial\phi_j^d}{\partial x_m}\left|\sigma_l\,\frac{V}{4c^2-2V}\right|\frac{\partial\phi_j^d}{\partial x_n}\right\rangle, \tag{6}$$

where again in the last step partial integration has been used. In the Pauli approximation spin–orbit matrix elements arise of the following form:

$$i\sum_{lmn}\epsilon_{lmn}\left\langle\frac{\partial\phi_i^d}{\partial x_m}\left|\sigma_l\,\frac{V}{4c^2}\right|\frac{\partial\phi_j^d}{\partial x_n}\right\rangle. \tag{7}$$

Compared to this matrix, the ZORA spin–orbit matrix is regularized by the potential in the numerator, which makes it effectively a $1/r$ potential close to a nucleus, whereas the Pauli spin–orbit operator behaves effectively like a $1/r^3$ potential.

A double-group symmetry adapted function can be written as a spatial function times spin α plus a spatial function times spin β

$$\phi_i^d(\mathbf{r},s)=\phi_i^{\alpha}(\mathbf{r})\,\alpha+\phi_i^{\beta}(\mathbf{r})\,\beta. \tag{8}$$

The spin integration can be done easily using the Pauli spin matrices. The spatial matrix elements are then given by

$$i\sum_{mn}\epsilon_{lmn}\left\langle\frac{\partial\phi_i}{\partial x_m}\left|\frac{V}{4c^2-2V}\right|\frac{\partial\phi_j}{\partial x_n}\right\rangle. \tag{9}$$

The double-group orbitals are constructed using the method of Snijders *et al.*[16,17] For the calculation of the scaled SR ZORA orbital energies [see Eq. (4)] we need matrix elements of the form

$$\langle\phi_i|\mathbf{p}\,\frac{c^2}{(2c^2-V)^2}\,\mathbf{p}|\phi_j\rangle=\sum_k\left\langle\frac{\partial\phi_i}{\partial x_k}\left|\frac{c^2}{(2c^2-V)^2}\right|\frac{\partial\phi_j}{\partial x_k}\right\rangle. \tag{10}$$

Finally for the calculation of the fully relativistic scaled ZORA orbital energies [see Eq. (3)] we need the matrix elements

$$\langle \phi_i^d | \boldsymbol{\sigma}\cdot\mathbf{p}\, \frac{c^2}{(2c^2-V)^2}\, \boldsymbol{\sigma}\cdot\mathbf{p} | \phi_j^d \rangle$$

$$= \langle \phi_i^d | \mathbf{p}\, \frac{c^2}{(2c^2-V)^2}\, \mathbf{p} | \phi_j^d \rangle$$

$$+ \langle \phi_i^d | \boldsymbol{\sigma}\cdot\boldsymbol{\nabla}\left(\frac{c^2}{(2c^2-V)^2} \right) \times \mathbf{p}) | \phi_j^d \rangle. \quad (11)$$

The first term is already present in the SR ZORA case. The last term can be written as (the gradient of a constant is zero)

$$\langle \phi_i^d | \boldsymbol{\sigma}\cdot\boldsymbol{\nabla}\left(\frac{c^2}{(2c^2-V)^2} \right) \times \mathbf{p}) | \phi_j^d \rangle$$

$$= \langle \phi_i^d | \boldsymbol{\sigma}\cdot\boldsymbol{\nabla}\left(\frac{V(4c^2-V)}{4c^2(2c^2-V)^2} \right) \times \mathbf{p}) | \phi_j^d \rangle$$

$$= i \sum_{lmn} \epsilon_{lmn} \left\langle \frac{\partial \phi_i^d}{\partial x_m} \middle| \sigma_l \frac{V(4c^2-V)}{4c^2(2c^2-V)^2} \middle| \frac{\partial \phi_j^d}{\partial x_n} \right\rangle. \quad (12)$$

All of the matrix elements needed in the scalar relativistic, fully relativistic, and scaled ZORA cases, can be calculated straightforwardly if one uses three-dimensional (3D) numerical integration. We use the 3D numerical integration method by the Velde and Baerends,[18] which can achieve high numerical precision. In the relativistic case it is only required to calculate in each sample point, in addition to the values of the basis functions, the derivatives of the basis functions with respect to the Cartesian coordinates $(\partial/\partial x, \partial/\partial y, \partial/\partial z)$. The 3D integration is particularly simple since the potential V is local in the Kohn–Sham form of density functional theory.

We note that the matrix elements needed in the scaled ZORA case are not more difficult to calculate than the ones that are needed for the unscaled ZORA kinetic energy. These matrix elements have to be calculated only once since the scaled ZORA orbital energies only have to be calculated after self-consistency is reached.

The calculation of differences in energies (bond energies) requires some precautions when using numerical integration. We use the ZORA ESA method described in some detail in Ref. 4, because it is easy and accurate.

III. ATOMIC GROUND STATE ENERGIES

The Hohenberg–Kohn theorem for nondegenerate ground states, that establishes a one-to-one relationship between the ground state density and the energy, can be extended in the case of degenerate ground states to a many-to-one mapping of the set of ground state densities, corresponding to the manifold of ground states, onto the ground state energy. However, the treatment of degenerate ground states is somewhat problematic since the present day approximate functionals are not invariant over the set of ground state densities. As a simple example, consider a hydrogen atom with a p^1 configuration. The density functionals currently in use will not give the same energy when the electron is placed in the $Y_l^{m=0}(p_z)$ orbital or when it is placed in the $Y_l^{m=1}((p_x+ip_y)/\sqrt{2})$ orbital. Sometimes a spherically averaged density with 1/3 electron each in p_x, p_y, and p_z, is chosen, which will give yet another energy. These ambiguities are numerically significant. For the boron atom, with a $(2p)^1$ shell, the atom with occupied $Y_l^{m=0}$ is 0.2 eV and with occupied $Y_l^{m=1}$ 0.07 eV below the spherically averaged atom. For the F atom with one hole in the $2p$ shell, the difference between a spherically averaged hole and a hole in the p_z atomic orbital is 0.3 eV. The problem already arises if there is only spin degeneracy, since the current functionals are not invariant under spin rotation. If one applies unrestricted (spin polarized) density functionals, in general different results are obtained if the electron is placed in some spatial orbital with spin α or with a mixed spin state $(\alpha+\beta)/\sqrt{2}$, although these states are of course degenerate. It is common practice to take only the state which is purely spin α or β. However, the problem becomes acute in relativistic calculations, where symmetry requirements will dictate spin mixing. If we adapt the atomic one-electron states to double-

TABLE I. Energy differences (in eV) between the atomic $|LS\rangle$ ground state in $L-S$ coupling ($L-S$ coupling column), and the $|JM_J\rangle$ ground state in intermediate coupling (Intermediate coupling column) with respect to the average-of-configuration energy (see the text). The third column gives the SO coupling constants used in the intermediate coupling calculation.

	$L-S$ coupling		Intermediate coupling		SO coupling constant	
	LDA	GGA	LDA	GGA	LDA	GGA
H	−0.90	−0.95	−0.90	−0.95	0.00	0.00
O	−1.58	−1.96	−1.59	−1.97	0.02	0.02
F	−0.41	−0.72	−0.43	−0.74	0.04	0.04
Te	−0.52	−0.71	−0.92	−1.09	0.54	0.53
I	−0.11	−0.19	−0.45	−0.52	0.68	0.66
Au	−0.15	−0.20	−0.15	−0.20	0.00	0.00
Tl	−0.13	−0.23	−0.83	−0.91	0.70	0.68
Pb	−0.48	−0.61	−2.04	−2.11	0.97	0.95
Bi	−1.10	−1.34	−2.14	−2.27	1.27	1.25

TABLE II. Optimized Slater exponents for all electron ZORA scalar relativistic calculations for iodine.

s		p		d		f	
n	ζ	n	ζ	n	ζ	n	ζ
1	1000.0	2	185.0	3	22.1	4	2.5
1	240.0	2	56.2	3	13.3	4	1.5
1	83.0	2	28.75	3	9.05		
1	53.5	2	21.25	4	7.23		
2	42.0	3	16.25	4	4.89		
2	29.5	3	12.2	4	3.40		
2	22.2	3	9.5	4	2.48		
3	13.25	4	9.55	5	2.00		
3	10.4	4	6.05				
4	8.55	4	4.25				
4	6.00	5	3.90				
4	4.45	5	2.60				
5	3.51	5	1.70				
5	2.44	5	1.12				
5	1.70						
6	1.40						

TABLE III. Bond length R_e and spin–orbit correction to the bond length $\Delta^{so}R_e$ in Å for some diatomic systems.

		I_2	Au_2	Bi_2	HI	AuH	TlH	IF	TlF	TlI	PbO	PbTe
Expt.[a]		2.667	2.472	2.661	1.609	1.524	1.870	1.910	2.084	2.814	1.922	2.595
ZORA	GGA	2.719	2.511	2.685	1.628	1.535	1.900	1.951	2.119	2.858	1.937	2.633
SR ZORA	GGA	2.697	2.517	2.655	1.625	1.535	1.931	1.940	2.126	2.872	1.939	2.629
$\Delta^{so}r_e$	GGA	0.022	−0.006	0.030	0.003	0.000	−0.031	0.011	−0.013	−0.014	−0.002	0.004
ZORA	LDA	2.670	2.452	2.637	1.624	1.526	1.868	1.919	2.073	2.783	1.910	2.588
SR ZORA	LDA	2.651	2.457	2.613	1.621	1.525	1.901	1.908	2.081	2.798	1.913	2.586
$\Delta^{so}r_e$	LDA	0.019	−0.005	0.024	0.003	0.001	−0.033	0.011	−0.008	−0.015	−0.003	0.002

[a]Reference 29.

group symmetry ($|jm_j\rangle$ states), the resulting states will no longer be pure spin states but will have the form of Eq. (8). The $p_{1/2}$ orbitals for instance lead to 1/3 density of one spin and 2/3 of the other spin. So in the limit where spin–orbit coupling becomes negligibly small and does not have any energetic effect, the simple linear transformation of the $|lsm_lm_s\rangle$ states to obtain $|jm_j\rangle$ states already causes a change in the approximate energy.

In order to obtain reasonable reference energies for the atomic ground states we have used the following approach. An established method to obtain multiplet splittings in open shell systems is the one suggested in Ref. 19, cf. also Refs. 20–22 (see for a recently proposed alternative Ref. 23). The method of Ref. 19 is based on the argument that it is only allowed to use current approximate exchange functionals for single determinantal states, since those states obey requirements for, e.g., the depth of the hole at the position of the reference electron that enters the derivation of the approximate functional. When working with single determinantal energies only one is essentially applying the diagonal sum method for obtaining multiplet energies which are well known from traditional atomic theory.[24] In this way the LS coupled states belonging to a configuration are obtained. This method we apply with the scalar relativistic ZORA Hamiltonian, obtaining LS energies with major relativistic effects (mass–velocity, Darwin) already included. In the next step the matrix elements of the spin–orbit operator may be evaluated between the LS states, so that the SO split and double–group adapted states can be obtained by diagonalization. A restriction to first-order spin–orbit splitting within individual LS terms is no longer justified in the heavy element compounds we are considering, so the full SO matrix is diagonalized over all LS terms arising from one $(nl)^p$ configuration (intermediate coupling). For details of this procedure we refer to the appendix. In Table I we present the resulting LS coupled and intermediate coupled ground state energies of the atoms needed in Sec. IV with respect to the average of the configuration energies, as well as spin–orbit constants used to obtain the intermediate coupled result.

IV. SPIN–ORBIT EFFECTS IN CLOSED SHELL MOLECULES

The effect of spin–orbit coupling has been studied in a series of diatomic molecules (see Tables III–VI) that represent different types of spin–orbit effects (see below). The self-consistent calculations on these molecules have been performed using the LDA potential. After convergence, density-gradient (GGA) corrections were calculated using the LDA density. We have noted that less than 0.01 eV difference exists for the dissociation energy between this ''post-self-consistent field (SCF)'' adding of the gradient corrections and a full SCF calculation with the gradient corrected exchange–correlation potential. For gold we use the all-electron large basis set B of Ref. 4. The hydrogen basis set is also described there. For thallium, lead, and bismuth we use basis sets optimized to numerical scalar relativistic ZORA orbitals, of the same size as the gold basis set, but with two extra 6p STO functions. In Table II the basis set for iodine is given. The tellurium basis set has the same size, with of course different optimized exponents. For oxygen and fluorine we use a triple 1s and quadruple valence basis set plus two 3d and two 4f polarization functions. The large basis sets used give an accuracy of better than 0.02 eV for the atomic valence orbital energies compared to numerical calculations, for both the ZORA and the SR ZORA calculations.

In Tables III–V results are given of all-electron molecu-

TABLE IV. Harmonic frequencies ω_e in cm^{-1} for some diatomic systems.

		I_2	Au_2	Bi_2	HI	AuH	TlH	IF	TlF	TlI	PbO	PbTe
Expt.[a]		215	191	173	2309	2305	1391	610	477	(150)	721	212
ZORA	GGA	197	178	174	2240	2270	1330	570	455	142	720	204
SR ZORA	GGA	210	177	193	2260	2270	1320	595	450	142	730	212
$\Delta^{so}\omega_e$	GGA	−6%	1%	−10%	−1%	0%	1%	−4%	1%	0%	−1%	−4%
ZORA	LDA	214	198	186	2260	2330	1390	610	490	155	755	216
SR ZORA	LDA	226	196	203	2280	2330	1370	630	485	155	765	223
$\Delta^{so}\omega_e$	LDA	−5%	1%	−8%	−1%	0%	1%	−3%	1%	0%	−1%	−3%

[a]Reference 29.

TABLE V. Molecular energies in eV with respect to the scalar relativistic atomic average-of-configuration (AOC) atomic energies (SR-ZORA calculations), or the fully relativistic average-of-configuration SO-AOC energies (ZORA calculations), see the text. Δ^{so} denotes the difference between the fully relativistic (ZORA) and scalar relativistic (SR ZORA) results.

		I_2	Au_2	Bi_2	HI	AuH	TlH	IF	TlF	TlI	PbO	PbTe
ZORA	GGA	2.62	2.71	6.52	4.71	4.52	3.96	4.31	6.37	4.14	8.23	5.74
SR ZORA	GGA	2.51	2.65	5.42	4.68	4.48	3.84	4.21	6.37	4.04	8.08	5.38
Δ^{so}	GGA	0.11	0.06	1.10	0.03	0.04	0.12	0.10	0.00	0.10	0.15	0.36
ZORA	LDA	3.07	3.29	7.11	4.99	4.87	4.12	4.85	6.83	4.53	8.88	6.28
SR ZORA	LDA	2.96	3.22	6.00	4.96	4.83	3.97	4.75	6.83	4.41	8.72	5.91
Δ^{so}	LDA	0.11	0.07	1.11	0.03	0.04	0.15	0.10	0.00	0.12	0.16	0.37

lar calculations on some diatomic compounds. First we have to note that the spin–orbit effect for most molecular properties is not large for these closed shell systems. The spin orbit effect on the bond distance never exceeds 0.03 Å, on frequencies it is less than 10%, and the molecular spin–orbit effect on the energies is in most cases less than 0.15 eV, except for Bi_2 and PbTe. In Table V these molecular energies are taken with respect to spherically and spin averaged (and for the fully relativistic ZORA, spin–orbit averaged) atoms. The ZORA results of Table V therefore reflect *molecular* spin–orbit coupling effects. The important *atomic* spin–orbit coupling effects, exemplified by the difference between the first and second columns of Table I, have to be taken into account in the molecular dissociation energies. The molecular D_e values, given in Table VI, will be discussed below, but first the molecular spin–orbit effects will be discussed with the help of Tables III–V.

In the literature many discussions exist rationalizing spin–orbit effects, especially in the context of *ab initio* calculations using relativistic effective core potentials (ECP), see, e.g., the reviews of Pitzer[25] and Ermler *et al.*[26] In particular spin–orbit interaction was analyzed in terms of the bonding between the spin–orbit split (jj coupled) atomic spinors as a starting point. Here we will use the scalar relativistic approximation as our starting point and we will discuss how the molecular orbitals are modified by the presence of the spin–orbit interaction.

For the lighter atoms, hydrogen, oxygen, and fluorine, the spin–orbit effect may be neglected, compared to the much larger spin–orbit effect in the heavier atoms. Also the first-order effect of spin–orbit coupling for closed shell systems is zero. We therefore expect fairly small effects of the spin–orbit coupling in these closed shell molecules compared to the open shell atoms. The spin–orbit effects will come from higher order effects, notably spin–orbit interaction between occupied and empty shells. The spin–orbit effects in Tables III–V can for a large part be understood by focusing on the molecular bonding and antibonding orbitals coming from the atomic valence p electrons. In Fig. 1 the one-electron molecular orbital levels coming from these orbitals for Bi_2 are schematically shown. At the left-hand side of Fig. 1 the scalar relativistic energies are shown and on the right-hand side the first-order effect of the spin–orbit interaction is included. The bonding π_u orbital will split due to this first-order spin–orbit effect, but since the split levels are both fully occupied, there is no net first-order spin–orbit effect. The effects should therefore come from off-diagonal spin–orbit interaction, which is only possible for orbitals with the same j and for homonuclear diatomics with the same inversion symmetry. There is only a net effect of this off-diagonal spin–orbit interaction if it is between an occupied and an unoccupied orbital, in which case it always has a stabilizing effect on the energy. Thus, for the levels shown in Fig. 1, we have off-diagonal spin–orbit interaction between the occupied bonding $\sigma_{1/2g}$ orbital and the unoccupied antibonding $\pi_{1/2g}$ orbital and between the occupied bonding $\pi_{1/2u}$ orbital and the unoccupied antibonding $\sigma_{1/2u}$ orbital. The effect of the off-diagonal spin–orbit interaction between orbitals will be larger if the difference in energy of these orbitals is smaller. For Bi_2 the bonding and antibonding orbitals will become closer in energy if we increase the distance between the atoms. Thus spin–orbit coupling will in this case have a flattening effect on the bond energy curve and an increasing effect on the bond length. Since there is a maximum number of interactions possible—each occupied orbital can be stabilized by interaction with an unoccupied one—and both atoms in the diatomic have a large spin–orbit coupling constant, the spin–orbit effect will be relatively large, as is indeed observed in tables III–V, in particular for the energetic stabilization.

TABLE VI. Molecular dissociation energies D_e in eV for some diatomic systems.

		I_2	Au_2	Bi_2	HI	AuH	TlH	IF	TlF	TlI	PbO	PbTe
Expt.[a]		1.56	2.31	2.03	3.20	3.36	2.06	2.92	4.60	2.77	3.87	2.57
ZORA	GGA	1.58	2.31	1.98	3.24	3.37	2.10	3.05	4.72	2.71	4.15	2.54
SR ZORA	GGA	2.13	2.25	2.74	3.54	3.33	2.66	3.30	5.42	3.62	5.51	4.06
ZORA	LDA	2.17	2.99	2.83	3.64	3.82	2.39	3.97	5.57	3.25	5.25	3.32
SR ZORA	LDA	2.74	2.92	3.80	3.95	3.78	2.94	4.23	6.29	4.17	6.66	4.91

[a]Reference 29.

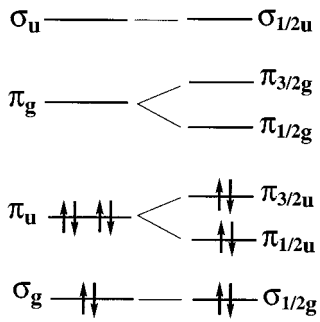

FIG. 1. Scalar relativistic (left-hand side) and first-order spin–orbit split (right-hand side) valence molecular orbital levels for Bi_2.

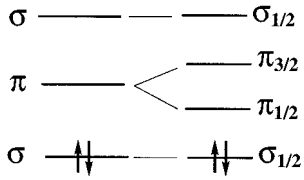

FIG. 2. Scalar relativistic (left-hand side) and first-order spin–orbit split (right-hand side) valence molecular orbital levels for TlH.

For the iodine molecule I_2 we can use Fig. 1 if we also fully occupy the antibonding π_g orbital. Now we only have to consider the off-diagonal spin–orbit interaction between the occupied bonding $\pi_{1/2u}$ orbital and the unoccupied antibonding $\sigma_{1/2u}$ orbital. As for Bi_2 the spin–orbit effect will be enhanced, if we increase the distance between the atoms, since the bonding and antibonding orbitals come closer in energy. The trends are therefore similar as in Bi_2, but they are, due to the smaller so coupling constant, smaller, in particular for the energy.

For the gold dimer Au_2 the spin–orbit effect is small, since the bonding is mainly due to the atomic $6s$ orbitals, which are not affected by spin–orbit coupling. The remaining small effect comes from the mixing of some $6p$ character into the $(6s+6s)$ bonding orbital, and the mixing of $6s$ character into almost fully occupied $5d$ shells. As a result spin–orbit coupling can have some effect. At larger distances between the gold atoms there is less $6p$ mixing, which reduces the spin–orbit effect, and consequently diminishes the spin–orbit stabilization. Therefore spin–orbit coupling will (very) slightly shorten the bond length of Au_2 and increase its binding energy and harmonic frequency.

We now turn to the heteronuclear compounds. Again the net first-order effect of spin–orbit coupling for these closed shell compounds is zero. The off-diagonal spin–orbit interaction between two orbitals only can become large if they have atomic character belonging to the same atom with the same l value ($l \neq 0$) and there is only a net effect if there is off-diagonal spin–orbit interaction between occupied and unoccupied orbitals.

For TlF, TlI, PbO, and PbTe, we have the same levels and occupation, coming from the valence atomic p orbitals, as in Fig. 1, except that they are not labeled by g or u anymore. This means that there are now more possibilities for off-diagonal spin–orbit interaction than in the homonuclear case. The relative position of the levels of the occupied bonding π and σ orbital are reversed for some of these compounds compared to the position they have in Fig. 1, the unoccupied antibonding π and σ orbital are always at the same relative position as in Fig. 1. For TlF, TlI, PbO, and PbTe, the occupied bonding orbitals have more character of the lighter, more electronegative element, whereas the unoccupied antibonding orbitals have more Tl or Pb character. If the distance between the atoms is increased, close to the equilibrium bond length, the occupied bonding orbitals will even be more biased toward the more electronegative element. Due to this effect the off-diagonal spin–orbit interaction is smaller at longer distances. This first effect of increasing the distance is larger if the difference in electronegativity of the two atoms is larger, like in TlF and TlI. A second effect of increasing the distance between the atoms, close to equilibrium, is that the bonding and antibonding orbitals will get closer in energy, which will increase the effect of the off-diagonal spin–orbit interaction. For PbO and PbTe there is some competition between these two effects, so that the spin–orbit effect on the bond distance is small. For TlF and TlI the first effect is dominating and spin–orbit coupling shortens the bond distance. The spin–orbit effect on the energy of these four compounds is largest for PbTe, since both lead and tellurium have a large effective spin–orbit parameter and the difference in electronegativity is the smallest for these atoms.

Compared to the previous compounds, IF also has a fully occupied antibonding π orbital. The off-diagonal spin–orbit interaction will be largest between the occupied antibonding $\pi_{1/2}$ orbital and the unoccupied antibonding $\sigma_{1/2}$. Both have more iodine than fluorine character, and acquire more iodine character with increasing distance. The two spin–orbit effects, which result from an increase in the distance between the atoms, are now in the same direction and will lengthen the bond distance.

In Fig. 2 the one-electron molecular orbital levels of TlH coming from the $1s$ orbital of hydrogen and the $6p$ orbitals of thallium are schematically shown. The bonding σ orbital ($H\ 1s+Tl\ 6p_\sigma$) has more hydrogen character. The energy of the nonbonding π orbital (thallium $6p_\pi$) will not change much if we increase the distance. In this case the first effect (decreasing SO interaction due to the increasing H character in the bonding orbital upon bond lengthening) is dominating, and spin–orbit coupling will shorten the bond length. For HI we can use Fig. 2 if we also fully occupy the π orbital, introducing occupied $\pi_{1/2}$ with unoccupied $\sigma_{1/2}$ SO interaction. Like in IF the first effect of the spin–orbit interaction will lengthen the bond distance. For AuH the spin–orbit effect is small, since the bonding effect is mainly due to atomic s orbitals, which are not affected by spin–orbit coupling. The bonding orbital now has almost no gold $6p$ character, which was responsible for part of the effect in Au_2.

Considering the bond distances (see also Fig. 3) we note that compared to experiment the ZORA GGA bond distances are too long, from 0.011 Å for AuH to 0.044 Å for TlI. The

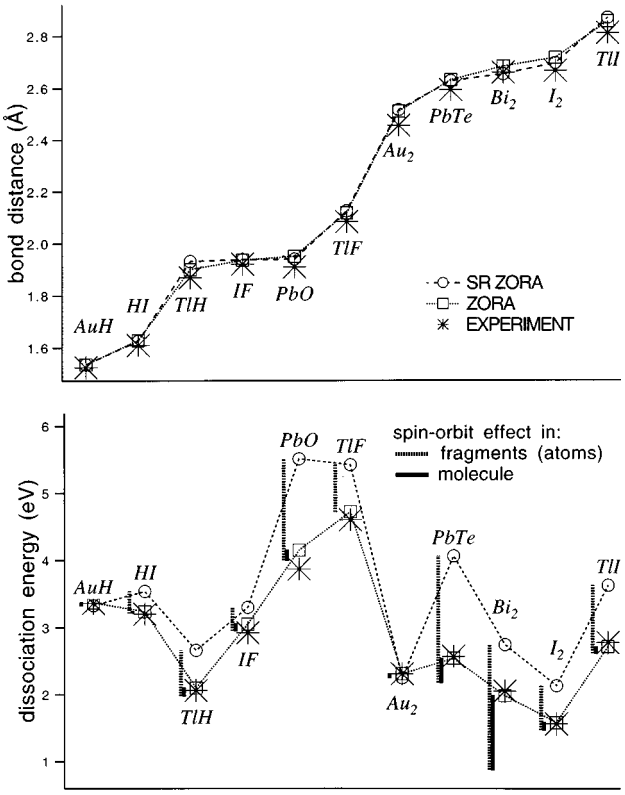

FIG. 3. Dissociation energies for some diatomic systems from all-electron (SR) ZORA GGA calculations.

SR ZORA GGA results lie between -0.006 Å for Bi_2 and $+0.061$ for TlH. The spin–orbit calculated results seem to give a more systematic deviation from experiment than the scalar relativistic results, especially the compounds where the spin–orbit coupling has its largest effect, namely Bi_2 and TlH, are better in line with the other molecules. The LDA results do not show a systematic overestimation of bond lengths. The theoretical ZORA LDA results deviate from experiment between -0.031 Å for TlI and $+0.015$ for HI. For the SR ZORA result this is between -0.048 Å for Bi_2 and $+0.031$ for TlH. The best agreement with experimental bond distances is usually found for the LDA results, with the only (marginal) exception for Bi_2.

For the harmonic frequencies we can do the same analysis. For most of these diatomics the spin–orbit coupling has a flattening effect on the bonding curve and vice versa. The flattening of the curve due to spin–orbit coupling can be quite large, especially for Bi_2 and I_2 and to a lesser extent for IF and PbTe. Usually the LDA frequencies are higher than the GGA ones, and the lowering due to the SO effect brings the LDA frequencies quite close to experiment. So the LDA frequencies are usually better than the GGA ones, with only Bi_2 and PbO as notable exceptions.

In order to identify the genuinely molecular spin–orbit effect on the energy we have to consider the results presented in Table V. In this table we can see the consequence of the fact that in first order the molecular spin–orbit effect is zero for these closed shell compounds. In most cases the molecular spin–orbit effect is less than 0.15 eV. Compared to the considerable SO effects in the atoms, the SO effect in the compounds containing Te, I, Tl, Pb, or Bi is relatively small. This exemplifies the well-known molecular quenching of the SO effect. This is basically due to the lifting of the atomic degeneracy of an nl set of atomic orbitals (AOs) due to the orbital interactions providing the molecular bonding. For instance, the stronger σ bonding than π bonding will usually shift the σ molecular orbitals (MOs) away from π MOs, which strongly diminishes the SO interaction. Moreover, the levels that remain degenerate, such as the π MOs, are usually fully occupied (or unoccupied), leaving no net first-order so effect. Examples of *partial* SO quenching by chemical bonding may be found in Refs. 27 and 28.

In a few instances, the molecular SO effect is sizable: for PbTe it is 0.36 eV and for Bi_2 it is even 1.1 eV. The relatively large effect on the energy for Bi_2 can be understood, considering the large effective spin–orbit parameter of bismuth, and the fact that the diagonal spin–orbit effect on the $\pi_{1/2g}$ orbital pushes its energy toward the $\sigma_{1/2g}$ such that off-diagonal spin–orbit coupling has large effects.

In Table VI the molecular dissociation energies are shown where in the scalar relativistic ZORA case the atomic reference energies are those of the lowest LS state, and in the fully relativistic ZORA case those of the lowest $|JM_J\rangle$ state obtained in intermediate coupling. The correction terms were taken from Table I. The ZORA GGA calculations give very accurate dissociation energies compared with experiment, the largest difference is 0.3 eV for PbO. They are the most accurate ones without exception. The SR ZORA GGA results for Au_2 and AuH are already accurate, since neither the molecule nor its fragments exhibit strong spin–orbit coupling effects. For the other compounds the omission of SO coupling in the scalar relativistic GGA calculation leads to a sizable deviation from experiment, ranging from 0.3 eV (HI) to 1.6 eV (PbO) too strong bonding. The reason for this lies almost entirely in the spin–orbit effect of the atoms. If we would only apply the atomic corrections obtained in intermediate coupling, while still using the scalar relativistic molecular results, the results would already improve considerably, to an accuracy of better than 0.2 eV except for PbTe (deviation of 0.4 eV) and Bi_2 (deviation of 1.1 eV). These are exactly the molecules which have a large molecular spin–orbit correction in the energies (see Table V). In Fig. 3 these results are shown in a form that clearly exhibits the atomic and molecular spin–orbit effects on the dissociation energy.

The ZORA LDA results for the molecular dissociation energies exhibit 0.3–1.4 eV too strong bonding compared to experiment. The situation that we find for these relativistic systems, of significant improvement resulting from the use of the GGA for bond energies, but no improvement or even slight worsening of the results for distances and frequencies, is well known in the nonrelativistic case.

In Table VII we have collected some results from the recent literature, where calculations, using spin–orbit coupling, are compared with scalar relativistic calculations. The spin–orbit effect for the bond distance and harmonic fre-

TABLE VII. Comparison with results from correlated relativistic calculations using ECPs, where the SO effect is calculated, for I_2,[a] for Bi_2,[b] for HI, and TlH.[c]

	I_2	Bi_2	HI	TlH
r_e (Å)				
SO	2.77	2.768	1.616	1.925
SR	2.75	2.734	1.614	1.953
ω_e (cm^{-1})				
SO	185	153	2331	1329
SR	199	165	2340	1310
D_e (eV)				
SO	0.76	1.49	2.88	2.32
SR	1.38		3.15	2.41

[a]Reference 30.
[b]Reference 31.
[c]Reference 32.

quencies are in close agreement to our findings. The literature values for the spin–orbit effects on the dissociation energy for I_2 (0.62 eV) and HI (0.27 eV) are close to our 0.55 and 0.30 eV, although our absolute values for D_e are much closer to experiment, in particular for I_2. For TlH there is considerable difference between our SO effect and the one obtained in Ref. 32. We find a large spin–orbit effect (0.56 eV), mainly due to the large spin–orbit effect on the energy of the thallium atom, whereas in Ref. 32 only a small effect (0.09 eV) is found. We do not have an explanation for this discrepancy. Usually, the atomic effect dominates, as for instance noted for I_2 in both the work of Schwerdtfeger *et al.*,[43] and Teichteil and Pélissier.[30] The situation with respect to the molecular so effect is not so clear. Schwerdtfeger *et al.* determine this effect as the difference in total energy between two pseudopotential calculations, one with a spin–orbit averaged pseudopotential and the other one with a pseudopotential including SO coupling (j dependent). These authors calculated the molecular spin–orbit effect in the dissociation energy to be 0.06 eV for HI and 0.14 eV for I_2, which can be compared with our 0.03 and 0.11 eV, respectively. However, Teichteil and Pelissier applied SO coupling in the configuration-interaction (CI) step, after a spin–orbit averaged pseudopotential calculation to generate the reference configurations, and find less than 0.01 eV. They ascribe the difference from Schwerdtfeger *et al.* to the use by the latter authors of essentially a $j-j$ coupling scheme for the molecule. The differences between the various molecular SO effects are still small in an absolute sense and may also be partly due to the different definitions, i.e., different procedures to calculate them, or even differences in the pseudopotentials. We note that for the bond distance, which can be calculated straightforwardly, Schwerdtfeger *et al.* find an increase in bond length for I_2 of 0.015 and for HI 0.003 Å due to spin–orbit coupling, comparable to, respectively, 0.02 and 0.003 Å from our calculations, and to the results of Teichteil and Pelissier.[30]

In Table VIII we present selected results from the litera-

TABLE VIII. Selection of results taken from the literature for the bond length r_e, harmonic frequency ω_e, and dissociation energy D_e for some diatomics compared to our ZORA GGA results.

	I_2	Au_2	HI	AuH	IF	TlF	PbO
r_e (Å)							
Expt.[a]	2.667	2.472	1.609	1.524	1.910	2.084	1.922
ZORA GGA	2.719	2.511	1.628	1.535	1.951	2.119	1.937
	2.73[b]	2.537[c]	1.598[d]	1.525[e]	1.916[f]	2.04[g]	1.893[h]
	2.71[b]	2.466[i]	1.601[j]	1.505[i]	1.944[f]		1.882[k]
	2.690[f]		1.615[f]				
	2.711[f]		1.626[f]				
ω_e (cm^{-1})							
Expt.[a]	215	191	2309	2305	610	477	721
ZORA GGA	197	178	2240	2270	570	455	720
	205[b]	178[c]	2354[d]	2288[e]	621[f]	592[g]	785[h]
	214[b]	195[i]	2410[j]	2619[i]	624[f]		800[k]
			2334[f]				
			2309[f]				
D_e (eV)							
Expt.[a]	1.56	2.31	3.20	3.36	2.92	4.60	3.87
ZORA GGA	1.58	2.31	3.24	3.37	3.05	4.72	4.15
	1.49[b]	2.12[c]	2.03[j]	2.92[e]		3.86[g]	1.3[k]
	1.69[b]	2.88[i]	3.09[f]	3.75[i]			3.5–3.8[k]
	1.43[f]		2.99[f]				
	1.42[f]						

[a]Reference 29.
[b]Reference 33.
[c]Reference 34.
[d]Reference 35.
[e]Reference 36.
[f]Reference 37.
[g]Reference 38.
[h]Reference 39.
[i]Reference 40.
[j]Reference 41.
[k]Reference 42.

TABLE IX. Dipole moments μ_e in D for some diatomic systems for the experimental geometry. Positive values mean A^+B^-.

		HI	AuH	TlH	IF	TlF	TlI	PbO	PbTe
Expt.[a]		0.45			1.95	4.23	4.61	4.64	2.73
ZORA	GGA	0.41	1.08	1.15	1.77	3.74	3.74	4.28	2.71
SR ZORA	GGA	0.43	1.08	1.40	1.71	3.88	4.17	4.44	3.01
$\Delta^{so}\mu_e$	GGA	−0.02	−0.00	−0.25	0.06	−0.06	−0.43	−0.16	−0.30
ZORA	LDA	0.49	0.95	1.00	1.85	3.78	3.63	4.29	2.61
SR ZORA	LDA	0.51	0.95	1.28	1.78	3.91	4.07	4.46	2.91
$\Delta^{so}\mu_e$	LDA	−0.02	−0.00	−0.28	0.07	−0.07	−0.44	−0.17	−0.30

[a]Reference 29.

ture for the compounds under study. Dirac–Fock calculations were performed by Matsuoka *et al.*[41,42] on HI and PbO. For PbO they also calculated the dissociation energy using density functionals for correlation. Dyall[39] also reported on Dirac–Fock calculations on PbO. The dissociation energies calculated from Dirac–Fock calculations are not very accurate, correlation effects have to be included. The Douglas–Kroll transformation, in the scalar relativistic approximation, was used in coupled cluster calculations on AuH by Kaldor and Hess.[36] Their results show good agreement with experiment, although their D_e of 2.92 eV is somewhat further off from the experimental value of 3.36 eV than our 3.37 eV. The Douglas–Kroll transformation was also used in scalar relativistic LDA calculations on Au_2 and AuH by Häberlen and Rösch,[40] who obtained results close to our SR ZORA LDA results. Relativistic ECPs including spin–orbit coupling were used by Balasubramanian[38] in correlated calculations on TlF. The other results come from scalar relativistic ECP calculations including correlation. A general conclusion, which most of these references make, is that since relativistic effects and correlation effects are not additive, one should include correlation in relativistic calculations on systems containing heavy elements. This is especially true for the dissociation energies.

In Table IX we compare ZORA and SR ZORA for the dipole moments of the heteronuclear diatomics at the experimental geometry. In the GGA results we have used the GGA potential in the self-consistent calculations. Compared to experiment the ZORA, GGA and SR ZORA GGA results have an average deviation of about 10%. In Table X we also have calculated the dipole moments for the same systems as the theoretical (SR) ZORA geometry of Table III. The deviations from experiment are reduced. Except for IF and PbTe the scalar relativistic results are closer to the (known) experimental values than the spin–orbit results, with an average deviation of approximately 5% for SR ZORA GGA and 7% for ZORA GGA. Considering the effect of spin–orbit coupling on the dipole moments, we note that there is a correlation with the changes in dipole moment and the changes in atomic electron affinity and ionization potential that we will result from spin–orbit coupling. For hydrogen, oxygen, fluorine, and gold the spin–orbit effect may be neglected. To remove an electron from thallium and lead will cost more energy in the spin–orbit case than in the scalar relativistic case. In the same way as the spin–orbit case, the gain in energy is less if we add an electron to tellurium or iodine, and it is less expensive to remove an electron from iodine than in the scalar relativistic case. With this in mind we can understand the spin–orbit effects on the dipole moments for these compounds: almost no effect for AuH, a lowering effect for HI, TlH, TlF, TlI, PbO, and PbTe, and an increasing effect on IF. A more detailed analysis may be based on the character of the valence molecular orbitals, much the same as we did before. The first-order effect of the spin–orbit interaction does not give a different density. For TlF, TlI, PbO, and PbTe, off-diagonal spin–orbit interaction can only mix in unoccupied orbitals, which have more character on Tl or Pb. For IF the main off-diagonal spin–orbit interaction is between an occupied antibonding $\pi_{1/2}$ orbital and an unoccupied antibonding $\sigma_{1/2}$ orbital. The antibonding $\pi_{1/2}$ orbital has more iodine character than the antibonding $\sigma_{1/2}$ orbital, thus the spin–orbit effect decreases the charge on iodine. In TlH the occupied bonding $\sigma_{1/2}$ orbital of Fig. 2 will mix with the unoccupied thallium $\pi_{1/2}$ orbital, which has more thallium character, and in HI the occupied iodine $\pi_{1/2}$ orbital will mix with the unoccupied antibonding $\sigma_{1/2}$ orbital, which has more hydrogen character. These orbital mixings explain the observed spin–orbit effects.

In Ref. 49 the spin–orbit effect on the dipole moment for HI was calculated using correlated relativistic ECPs. At the experimental geometry they find it to be −0.019 D, which is the same as we have found. Dolg *et al.*[46] estimated the spin–

TABLE X. Dipole moments μ_e in D for some diatomic systems at the (SR) ZORA geometry from Table III.

		HI	AuH	TlH	IF	TlF	TlI	PbO	PbTe
Expt.[a]		0.45			1.95	4.23	4.61	4.64	2.73
ZORA	GGA	0.41	1.08	1.28	1.94	3.97	4.01	4.35	2.85
SR ZORA	GGA	0.43	1.09	1.69	1.83	4.16	4.54	4.53	3.14
$\Delta^{so}\mu_e$	GGA	−0.02	−0.01	−0.41	0.11	−0.19	−0.53	−0.18	−0.29

[a]Reference 29.

TABLE XI. Results taken from the literature for dipole moments μ_e in D for some diatomic systems. Positive values mean A^+B^-.

	HI	AuH	TlH	TlI	PbO	PbTe
Expt.[a]	0.45			4.61	4.64	2.73
	0.460[b]	2.04[c]	0.77[c]	4.85[c]	4.52–4.70[d]	3.22[c]
	0.40[e]	1.58[f]			3.74[g]	2.67[g]
		1.16[h]			5.389[i]	

[a]Reference 29.
[b]Reference 44.
[c]Reference 45.
[d]Reference 46.
[e]Reference 35.
[f]Reference 47.
[g]Reference 48.
[h]Reference 48.
[i]Reference 39.

orbit correction for PbO to be between -0.07 and -0.23 D, our theoretical result -0.16 lies in this range.

In Table XI we give some results for calculations of dipole moments taken from the literature. Reference 45 used Dirac–Fock calculations, except for AuH, where correlation effects were included. Dyall[39] also used Dirac–Fock calculations for PbO. The only relativistic LDA results in Table XI are from Häberlen *et al.*[40] for AuH. Their result for AuH is much closer to our result than the other two. The remaining results in Table XI come from calculations using relativistic ECPs. The results of Table XI show similar deviations from experiment as our results. Apparently it is difficult to calculate the dipole moments of these compounds with high accuracy.

V. CONCLUSIONS

In this paper we have calculated and rationalized the effect of spin–orbit coupling in a series of closed shell diatomic molecules. For the calculated compounds the spin–orbit effect on the bond distance never exceeded 0.03 Å, and on frequencies it is less than 10%. Also the molecular spin–orbit effect on the energies is often small, except for Bi_2 and PbTe. However, to obtain the spin–orbit effects on the dissociation energy it is absolutely necessary to take into account the effect of spin–orbit coupling in the constituent atomic fragments since it can be very large in these open shell systems. A method is proposed to obtain the ground state energy of open shell atoms, which uses present day density functionals in an intermediate coupling scheme. This method is used for the calculation of some atomic multiplet splittings and it is shown to give realistic energy differences. Using these intermediate-coupling atomic energies for the calculation of the dissociation energies of the compounds under study, we obtain high accuracy if we include gradient correction (GGA) terms in the energy. The ZORA GGA results are within 0.15 eV from experiment, with only one exception for PbO (0.28 eV). For most compounds, except for Bi_2 and PbTe, this accuracy in the dissociation energy could be obtained by only taking into account the spin–orbit effects in the atoms. For Bi_2 and PbTe it has been shown that, to obtain high accuracy, it is also necessary to take spin–orbit effects for the molecular energy into account. Except for these two molecules, in most cases the molecular spin–orbit effects are on the order of the accuracy of the calculations compared to experiment. The calculated dipole moments at the experimental geometry are still off by approximately 10% compared to the known experimental results in the both the spin–orbit and scalar relativistic case. They are improved (7% and 5% discrepancy, respectively) when calculated at the optimized geometries.

In complete analogy to the nonrelativistic case, we find that the gradient corrections reduce the overbinding of LDA, but do not improve bond distances and frequencies.

APPENDIX: THE CALCULATION OF ATOMIC MULTIPLET ENERGIES

There are a few details concerning the approach to calculating atomic multiplet energies in intermediate coupling sketched above that deserve some comment.

We define the average-of-configuration (AOC) orbitals and energy as resulting from a self-consistent field calculation with the electrons of the configuration distributed equally over all one-electron orbitals. This leads to fractional occupation numbers, a spherically symmetric density, and equal spin up and down densities. This is a convenient reference point, that can easily be reproduced by any atomic structure code. In Table I, the first column, we quote the scalar relativistic (LS coupled) ground state energies with respect to the scalar relativistic AOC energy for the atoms of interest. It is not difficult to identify determinants that are pure $|LSM_LM_S\rangle$ states belonging to the ground term and which therefore can be used to calculate the ground state energy. There remains the question whether one should employ the AOC orbitals in this determinant, or whether one should try to lower the energy further by trying to optimize the orbitals self-consistently for this particular determinant. A further choice would be whether to apply symmetry and equivalence restrictions between the orbitals of one nl shell, or to search for the lowest energy without any symmetry constraint. We have found that the use of optimized orbitals (essentially the lowest possible one-determinantal energy) lowers the energy of the ground state with respect to the use of AOC orbitals, which always obey the symmetry and equivalence restrictions, by less than 0.05 eV for the heavy elements we are dealing with. However, for the light (second row) elements the effect may amount to 0.15 eV. We have used the optimized results throughout, but it is clear that with the present unsatisfactory state of the density functional theory for open shell systems, one should consider these effects as ''error bars'' that have to be put on the calculated ground state energies. These error bars are virtually negligible—in view of the general accuracy of the results—for the heavy elements, but not so for the light elements.

In order to introduce SO coupling between the LS terms, we first need the scalar relativistic energies of all $L-S$ coupled states (not just the ground term) of the $(nl)^p$ configuration. These are calculated using the diagonal sum method of Ref. 19. There are also error bars in this procedure because of the above cited lack of certain invariance properties in the exchange–correlation functionals. There is also the question of the use of either converged orbitals or the

TABLE XII. Atomic multiplet energies in eV. Experimental results are taken from the tables of Moore.[a]

	$L-S$ coupling		Intermediate coupling			
	LDA	GGA	J	LDA	GGA	EXP
Tellurium						
$^3P_2$	0	0	2	0	0	0
$^3P_0$	0	0	0	0.61	0.62	0.58
$^3P_1$	0	0	1	0.67	0.64	0.59
$^1D_2$	0.70	0.88	2	1.23	1.37	1.31
$^1S_0$	1.94	2.24	0	2.68	2.90	2.88
Iodine						
$^2P_{1/2}$	0	0	1/2	0	0	0
$^2P_{3/2}$	0	0	3/2	1.02	0.99	0.94
Thallium						
$^2P_{1/2}$	0	0	1/2	0	0	0
$^2P_{3/2}$	0	0	3/2	1.05	1.02	0.97
Lead						
$^3P_0$	0	0	0	0	0	0
$^3P_1$	0	0	1	1.08	1.03	0.97
$^3P_2$	0	0	2	1.41	1.40	1.32
$^1D_2$	0.59	0.69	2	2.78	2.76	2.66
$^1S_0$	1.54	1.69	0	3.70	3.74	3.65
Bismuth						
$^4S_{3/2}$	0	0	3/2	0	0	0
$^2D_{3/2}$	0.88	1.03	3/2	1.49	1.48	1.42
$^2D_{5/2}$	0.88	1.03	5/2	1.91	1.97	1.91
$^2P_{1/2}$	1.58	1.72	1/2	2.61	2.66	2.69
$^2P_{3/2}$	1.58	1.72	3/2	4.08	4.08	4.11

[a]Reference 51.

AOC orbitals in the one-determinantal states. Since we use optimized orbitals for the ground state energies, we have used optimized orbitals throughout, noting that for the heavy elements this has negligible effects. We actually only need the calculated term energies for the heavy elements, since the SO coupling is too small in the light elements to cause non-negligible coupling of the ground state with higher LS states. The term energies at the scalar relativistic level for the heavy elements are shown in the first column of Table XII. The diagonal sum method is only used for Te, Pb, and Bi, since for I, Au, and Tl we only have one state in $L-S$ coupling for the lowest configuration.

In order to apply the spin–orbit interaction between the LS terms, we use the standard approach in atomic structure theory, see, e.g., Condon and Shortley.[50] The effect of spin–orbit coupling is summarized in an effective spin–orbit coupling constant ζ. There are several ways to obtain good estimates of this parameter. It is possible to calculate expectation values of the SO operator over AOC orbitals. Since we do not use the AOC orbitals for all LS multiplet states, but perform separate optimizations, we calculate an effective SO parameter, to be used for the SO interaction between all the LS terms, from the difference in energy between the lowest jj configuration and a SO-AOC calculation. In the latter the fully relativistic ZORA Hamiltonian is used and electron occupations are chosen in accordance with the scalar relativistic $(nl)^p$ parent configuration from which the LS terms arise. For p^2 this would mean an occupation of 2/3 electron in the $p_{1/2}$ shell, and 4/3 electrons in the $p_{3/2}$ shell (occupation 2/6 in each $|p1/2,m_j\rangle$ and each $|p3/2,m_j\rangle$ one-electron spinor). The lowest jj configuration would of course be $(p_{1/2})^2$. The resulting spin–orbit constants are given in Table I. Calculating a spin–orbit coupling constant from the expectation value of the spin–orbit operator over AOC orbitals does not lead to very different values. For Te and I the resulting spin–orbit coupling constant would only be a few hundredths of an eV smaller, for Tl, Pb, and Bi however it would be some 15% smaller.

As a consequence of the spin–orbit interaction the energy of the resulting $|JM_J\rangle$ ground state will be lower than the ground term in the LS spectrum of states. The second column of Table I shows the energy of the lowest $|JM_J\rangle$ with respect to the AOC energy. The energy lowering compared to the lowest LS state (column 1) is considerable in the atoms with large SO coupling constants. In Table XII the whole spectrum of $|JM_J\rangle$ states resulting from the SO coupling is shown, together with the experimental values.[51] Both LDA and the density gradient corrected (GGA) splittings are in close agreement with experiment, deviations are less than 0.1 eV. This accuracy is actually better than the error bars of the current density functionals for the SR $|LS\rangle$ multiplet energies, so it may be considered somewhat fortuitous. We have referred above to two types of AOC calculation, one scalar relativistic and the other one including so coupling. It is to be noted that these AOC calculations lead to different total energies, even if the first-order effect of the SO interaction within a manifold of spin–orbitals belonging to a $(nl)^p$ configuration, all equally occupied, would not lead to a change in energy. However, a full self-consistent calculation, including the SO operator, changes the SO-AOC energy with respect to the scalar relativistic AOC energy because higher order effects of the SO operator play a role, in particular in deep core fully occupied shells. This is already apparent if one considers the exact solutions in a hydrogenic heavy ion, for example the Uranium^{91+} ion. The averaged relativistic $2p$ orbital energy of -1045.54 a.u. (1/3 times -1257.39 $(2p_{1/2})$ plus 2/3 times -1089.61 $(2p_{3/2})$ is approximately 15 a.u. lower than the scalar relativistic orbital energy -1130.34 a.u. So even for closed shells SO interaction can be important, due to the second- and higher-order effects of the so coupling. The radial part of the $2p_{1/2}$ orbital is in that case not identical anymore to the radial part of the $2p_{3/2}$ orbital. We have, however, observed that the change in density of the core orbitals due to SO effects has very little effect on the valence orbitals.

Since the higher order SO energetic effects are significant, and since the fully relativistic all-electron calculations on molecules to be reported do include these SO effects in the deep core shells, we have to take care to include them in the atoms as well. This means that the atomic ground state energies to be used in the dissociation energy calculations of the molecules have to be obtained by taking the SO-AOC energies and adding the energy lowerings given in column 2 of Table I with respect to that reference point.

[1] Ch. Chang, M. Pélissier, and Ph. Durand, Phys. Scr. **34**, 394 (1986).
[2] J.-L. Heully, I. Lindgren, E. Lindroth, S. Lundqvist, and A.-M. Mårtensson-Pendrill, J. Phys. B **19**, 2799 (1986).
[3] E. van Lenthe, E. J. Baerends, and J. G. Snijders, J. Chem. Phys. **99**, 4597 (1993).
[4] E. van Lenthe, E. J. Baerends, and J. G. Snijders, J. Chem. Phys. **101**, 9783 (1994).
[5] R. van Leeuwen, E. van Lenthe, E. J. Baerends, and J. G. Snijders, J. Chem. Phys. **101**, 1272 (1994).
[6] J. G. Snijders and A. J. Sadlej, Chem. Phys. Lett. **252**, 51 (1996).
[7] A. D. Becke, Phys. Rev. A **38**, 3098 (1988).
[8] J. P. Perdew, Phys. Rev. B **33**, 8822 (1986).
[9] A. D. Becke, J. Chem. Phys. **96**, 2155 (1992).
[10] L. Fan and T. Ziegler, J. Chem. Phys. **94**, 6057 (1991).
[11] W. C. Ermler, Y. S. Lee, P. A. Christiansen, and K. S. Pitzer, Chem. Phys. Lett. **81**, 70 (1981).
[12] C. Teichteil, M. Pélissier, and F. Spiegelmann, Chem. Phys. **81**, 273 (1983).
[13] K. S. Pitzer and P. A. Christiansen, Chem. Phys. Lett. **77**, 589 (1981).
[14] K. S. Pitzer, Acc. Chem. Res. **12**, 271 (1979).
[15] A. J. Sadlej, J. G. Snijders, E. van Lenthe, and E. J. Baerends, J. Chem. Phys. **102**, 1758 (1994).
[16] J. G. Snijders, E. J. Baerends, and P. Ros, Mol. Phys. **38**, 1909 (1979).
[17] J. G. Snijders, Ph.D. thesis, Vrije Universiteit, Amsterdam, The Netherlands, 1979.
[18] G. te Velde and E. J. Baerends, J. Comput. Phys. **99**, 84 (1992).
[19] T. Ziegler, A. Rauk, and E. J. Baerends. Theor. Chim. Acta **43**, 261 (1977).
[20] U. von Barth, Phys. Rev. A **20**, 1693 (1979).
[21] M. Lannoo, G. A. Baraff, and M. Schlüter, Phys. Rev. B **24**, 943 (1979).
[22] J. H. Wood, J. Phys. B: At. Mol. Phys. **13**, 1 (1980).
[23] A. D. Becke, A. Savin, and H. Stoll. Theor. Chim. Acta **91**, 147 (1995).
[24] J. C. Slater, *Quantum Theory of Atomic Structure* (McGraw-Hill, New York, 1960), Vol. I.
[25] K. S. Pitzer, Int. J. Quantum Chem. **25**, 131 (1984).
[26] W. C. Ermler, R. B. Ross, and P. A. Christiansen, Adv. Quantum Chem. **19**, 139 (1988).
[27] P. M. Boerrigter, E. J. Baerends, and J. G. Snijders, Chem. Phys. **122**, 357 (1988).
[28] R. L. DeKock, E. J. Baerends, P. M. Boerrigter, and J. G. Snijders, Chem. Phys. Lett. **105**, 308 (1984).
[29] K. P. Huber and G. Herzberg, *Constants of Diatomic Molecules* (Van Nostrand Reinhold, New York, 1979), Vol. 4.
[30] C. Teichteil and M. Pélissier, Chem. Phys. **180**, 1 (1994).
[31] K. K. Das, H.-P. Liebermann, and R. J. Buenker, J. Chem. Phys. **102**, 4518 (1995).
[32] L. Seijo, J. Chem. Phys. **102**, 8078 (1995).
[33] D. Danovich, J. Hrusak, and S. Shaik, Chem. Phys. Lett. **233**, 249 (1995).
[34] P. Schwerdtfeger, Chem. Phys. Lett. **183**, 457 (1991).
[35] V. Kello and A. J. Sadlej, J. Chem. Phys. **93**, 8122 (1990).
[36] U. Kaldor and B. A. Hess, Chem. Phys. Lett. **230**, 1 (1994).
[37] M. N. Glukhovtsev, A. Pross, M. P. McGrath, and L. Radom, J. Chem. Phys. **103**, 1878 (1995).
[38] K. Balasubramanian, J. Chem. Phys. **82**, 3741 (1985).
[39] K. G. Dyall, J. Chem. Phys. **98**, 2191 (1993).
[40] O. D. Häberlen and N. Rösch, Chem. Phys. Lett. **199**, 491 (1992).
[41] O. Matsuoka, J. Chem. Phys. **97**, 2271 (1992).
[42] O. Matsuoka, L. Pisani, and E. Clementi, Chem. Phys. Lett. **202**, 13 (1992).
[43] P. Schwerdtfeger, L. v. Szentpaly, K. Vogel, H. Silberbach, H. Stoll, and H. Preuss, J. Chem. Phys. **84**, 1606 (1986).
[44] D. A. Chapman, K. Balasubramanian, and S. H. Lin, Phys. Rev A **38**, 6098 (1988).
[45] A. F. Ramos, N. C. Pyper, and G. L. Malli, Phys. Rev. A **38**, 2729 (1988).
[46] M. Dolg, A. Nicklass, and H. Stoll, J. Chem. Phys. **99**, 3614 (1993).
[47] A. J. Sadlej, J. Chem. Phys. **95**, 2614 (1991).
[48] V. Kello and A. J. Sadlej, J. Chem. Phys. **98**, 1345 (1993).
[49] D. A. Chapman, K. Balasubramanian, and S. H. Lin, J. Chem. Phys. **87**, 5325 (1987).
[50] E. U. Condon and G. H. Shortley, *The Theory of Atomic Spectra* (Cambridge University Press, Cambridge 1951).
[51] C. E. Moore, *Atomic Energy Levels: as Derived from the Analysis of Optical Spectral/Reissued* (National Bureau of Standards, Washington, 1971).